



LABORATORI NAZIONALI DI FRASCATI
SIS-Pubblicazioni

LNF-99/009(P)

26 Marzo 1999

INFNNA-IV-99/12
UWThPh-1999-19

$\eta \rightarrow \pi^+ \pi^- \pi^0 \gamma$ **in Chiral Perturbation Theory***

G. D'Ambrosio¹, G. Ecker², G. Isidori³ and H. Neufeld²

¹⁾ *INFN, Sezione di Napoli*

Dipartimento di Scienze Fisiche, Università di Napoli I-80126 Napoli, Italy

²⁾ *Institut für Theoretische Physik, Universität Wien*

Boltzmannngasse 5, A-1090 Wien, Austria

³⁾ *INFN, Laboratori Nazionali di Frascati, P.O. Box 13, I-00044 Frascati, Italy*

Abstract

We analyse the radiative decay $\eta \rightarrow \pi^+ \pi^- \pi^0 \gamma$ in the low-energy expansion of the Standard Model. We employ the notion of “generalized bremsstrahlung” to take full advantage of the theoretical and experimental information on the corresponding non-radiative $\eta \rightarrow 3\pi$ decay. The direct emission amplitude of $\mathcal{O}(p^4)$ is due to one-loop diagrams with intermediate pions (isospin violating) and kaons (isospin conserving). Vector meson contributions appearing at $\mathcal{O}(p^6)$ are also evaluated.

PACS: 13.40.-f, 12.39.Fe

Submitted to Physics Letters B

* Work supported in part by TMR, EC-Contract No. ERBFMRX-CT980169 (EURODAΦNE)

1. The decays $\eta \rightarrow 3\pi$ are forbidden in the limit of isospin conservation. Neglecting the small electromagnetic corrections [1], the amplitudes are proportional to the isospin breaking mass difference $m_u - m_d$. The leading-order amplitude in the low-energy expansion of $\mathcal{O}(p^2)$ [2] is known to receive large higher-order corrections, both at $\mathcal{O}(p^4)$ [3] and beyond [4,5].

The radiative decay $\eta \rightarrow \pi^+\pi^-\pi^0\gamma$ is in principle an interesting channel. At lowest order p^2 , the amplitude is pure bremsstrahlung. At next-to-leading order an additional contribution appears (direct emission) that is nonvanishing even in the isospin limit. Therefore, the direct emission amplitude carries in principle new information that is not accessible in $\eta \rightarrow 3\pi$ decays. The notion of a direct emission amplitude is not unique except that it starts at $\mathcal{O}(k)$ where k is the photon momentum. For instance, the so-called quadratic slope parameters of the non-radiative amplitude arising at $\mathcal{O}(p^4)$ also generate a radiative amplitude of $\mathcal{O}(k)$ that one may combine with the bremsstrahlung amplitude because it is also completely fixed by the non-radiative process. We have recently shown [6] that one can define a generalized bremsstrahlung (GB) amplitude for a generic radiative four-meson process that includes the effects of all local terms of $\mathcal{O}(p^4)$ contributing to the non-radiative transition.

The main advantages of the GB amplitude are:

- Since all local contributions to the non-radiative amplitude of $\mathcal{O}(p^4)$ are included, the uncertainties in the corresponding low-energy constants do not propagate to the direct emission amplitude (defined here as the difference between the total and the GB amplitudes).
- If there are substantial higher-order contributions beyond $\mathcal{O}(p^4)$ in the non-radiative amplitude they can be included in the GB amplitude by using the experimentally measured non-radiative amplitude. For $\eta \rightarrow \pi^+\pi^-\pi^0\gamma$, this is especially welcome because the unitarity corrections [4,5] modify both rate and slope parameters of $\eta \rightarrow 3\pi$ substantially. Using the experimental values in the GB amplitude allows for a much more accurate determination of the total amplitude.

The purpose of this letter is to calculate both GB and direct emission amplitudes for $\eta \rightarrow \pi^+\pi^-\pi^0\gamma$ along the same lines as for $K \rightarrow 3\pi\gamma$ [7]. We will comment on the differences between the GB and the usual bremsstrahlung amplitudes and we discuss the relative importance of the main contributions to direct emission: pion loops (isospin violating), kaon loops and vector meson exchange (both isospin conserving). The channel under consideration has already been studied in the framework of chiral perturbation the-

ory by Bramon et al. [8] where also references to the earlier literature can be found. We will discuss the differences to Ref. [8] as we go along.

At present, the Particle Data Group quotes an upper limit $B(\eta \rightarrow \pi^+\pi^-\pi^0\gamma) < 6 \times 10^{-4}$ [9]. However, the experimental situation will improve soon. For instance, at the Φ -factory DAΦNE in Frascati one expects [10] a total yield of 10^8 η per year.

2. To evaluate the bremsstrahlung contribution to $\eta \rightarrow \pi^+\pi^-\pi^0\gamma$ we need to know the amplitude for $\eta(p_\eta) \rightarrow \pi^+(p_+)\pi^-(p_-)\pi^0(p_0)$. Neglecting electromagnetic corrections [1], the amplitude can be written in the form [3]

$$A(s, s_\pm) = \frac{B(m_u - m_d)}{3\sqrt{3}F_\pi^2} \left(1 + 3\frac{s - s_0}{M_\eta^2 - M_\pi^2}\right) (1 + \delta(s, s_\pm)) \quad (1)$$

where B is a parameter of the lowest-order chiral Lagrangian [11] related to the quark condensate and $F_\pi = 92.4$ MeV is the pion decay constant. The kinematical variables s, s_\pm, s_0 are defined as

$$s = (p_\eta - p_0)^2, \quad s_\pm = (p_\eta - p_\pm)^2, \quad s_0 = \frac{1}{3}(s + s_+ + s_-). \quad (2)$$

The function $\delta(s, s_\pm)$ vanishes to lowest order p^2 . At $\mathcal{O}(p^4)$ it receives both loop and counterterm contributions [3]. Higher-order effects due to $\pi\pi$ rescattering are important and have been included in $\delta(s, s_\pm)$ by way of dispersion relations [4,5]. These higher-order corrections increase the rate of $\mathcal{O}(p^4)$ by some 25 ÷ 30 % and must be included for a reliable estimate of the bremsstrahlung amplitude.

Experimental results are conventionally expressed in terms of the Dalitz variables x, y defined as

$$x = \frac{\sqrt{3}(s_- - s_+)}{2M_\eta Q}, \quad y = \frac{3}{2M_\eta Q} [(M_\eta - M_{\pi^0})^2 - s] - 1, \quad (3)$$

$$Q = M_\eta - 2M_{\pi^+} - M_{\pi^0}.$$

Up to a normalization constant, the experimental Dalitz plot distribution is fitted by a function of the form [9,12]

$$A(x, y)^2 = A(0, 0)^2 (1 + ay + by^2 + cx^2) \quad (4)$$

where $A(x, y)$ corresponds to the decay amplitude (1). Charge conjugation invariance forbids a term linear in x .

The present experimental and theoretical status of the parameters in (4) is summarized in Table 1. We do not need a value for $A(0, 0)$ since we always normalize our results to

| | | a | b | c |
|---|---------|------------------|-----------------|------|
| Experiment | [9, 12] | -1.22 ± 0.07 | 0.22 ± 0.11 | — |
| Gasser and Leutwyler $\mathcal{O}(p^4)$ | [3] | -1.33 | 0.42 | 0.08 |
| Kambor et al. (solution a) | [4] | -1.16 | 0.24 | 0.09 |
| Kambor et al. (solution b) | [4] | -1.16 | 0.26 | 0.10 |

Table 1: Experimental and theoretical values of the linear and quadratic slopes of $\eta \rightarrow \pi^+ \pi^- \pi^0$ defined in Eq. (4).

the non-radiative decay. In this way, errors are substantially reduced. From Table 1, the importance of higher-order corrections is evident also for the slope parameters. For the numerical calculation, we will use the experimental values of a, b . Experiments have not been sensitive enough to extract the parameter c which is however relatively stable with respect to chiral corrections (we will take $c = 0.10$ for the numerics).

The kinematics of the decay $\eta(p_\eta) \rightarrow \pi^+(p_+) \pi^-(p_-) \pi^0(p_0) \gamma(k)$ is specified by adding the variables

$$t_i = k \cdot p_i \quad (i = \eta, +, -, 0) \quad (5)$$

with

$$t_\eta = t_+ + t_- + t_0 .$$

Any three of the t_i together with x and y in (3) form a set of independent variables.

With CP conserved, there is only an electric transition amplitude that we write as

$$A(\eta \rightarrow \pi^+ \pi^- \pi^0 \gamma) = e \varepsilon^\mu(k) E_\mu(x, y, t_i) \quad (6)$$

with

$$k^\mu E_\mu = 0 .$$

Low's theorem [13] relates the radiative amplitude to the corresponding non-radiative amplitude and their first derivatives with respect to the Dalitz variables up to $\mathcal{O}(k)$. For a general four-body amplitude $A(s, t)$ with Mandelstam variables s, t , both $\frac{\partial A(s, t)}{\partial s}$ and $\frac{\partial A(s, t)}{\partial t}$ contribute to the Low amplitude. Since there are two neutral particles in our process we can choose variables and assign particle labels such that only one of the derivatives enters. With the variables chosen in (3) and with $p_1 = -p_\eta, p_2 = p_0, p_3 = p_-$ and

$p_4 = p_+$ in the notation of Ref. [6], Low's theorem reads

$$\begin{aligned}
E_{\text{Low}}^\mu(x, y, t_i) &= A(x, y) \left(\frac{p_+^\mu}{t_+} - \frac{p_-^\mu}{t_-} \right) \\
&- \frac{\sqrt{3}}{M_\eta Q} \left[p_0^\mu + p_\eta^\mu - \frac{p_-^\mu}{t_-} (t_0 + t_\eta) \right] \frac{\partial A(x, y)}{\partial x} + \mathcal{O}(k).
\end{aligned} \tag{7}$$

To lowest order p^2 , the radiative amplitude is completely given by the Low amplitude (7). In fact, since there is no x -dependence in the $\eta \rightarrow 3\pi$ amplitude of $\mathcal{O}(p^2)$ in (1), only the non-derivative part in (7) contributes. Starting at $\mathcal{O}(p^4)$, an x -dependence is generated that produces the quadratic slope term cx^2 in (4).

However, one can do better than that. In order to account for all the local parts of $\mathcal{O}(p^4)$ in the non-radiative amplitude that contribute also to the radiative amplitude, a so-called generalized bremsstrahlung amplitude can be introduced [6]. One major advantage of using the GB amplitude is that the remaining direct emission amplitude $E^\mu - E_{\text{GB}}^\mu$ can only receive contributions from local terms of $\mathcal{O}(p^4)$ that do not contribute to the non-radiative amplitude. For $\eta \rightarrow \pi^+\pi^-\pi^0\gamma$, only the low-energy constant L_9 [11] could therefore appear in the direct emission amplitude. However, the corresponding counterterm does not contribute to $\eta \rightarrow \pi^+\pi^-\pi^0\gamma$ even for $m_u \neq m_d$. Thus, the one-loop contribution to direct emission is necessarily finite.

The general formula for the GB amplitude of Ref. [6] simplifies in the present case to

$$\begin{aligned}
E_{\text{GB}}^\mu &= A(x, y) \left(\frac{p_+^\mu}{t_+} - \frac{p_-^\mu}{t_-} \right) \\
&- \frac{\sqrt{3}}{M_\eta Q} \left[p_0^\mu + p_\eta^\mu - \frac{p_-^\mu}{t_-} (t_0 + t_\eta) \right] \frac{\partial A(x, y)}{\partial x} \\
&+ \frac{3}{2M_\eta^2 Q^2} \left\{ (t_0 + t_\eta) \left[p_0^\mu + p_\eta^\mu - \frac{p_-^\mu}{t_-} (t_0 + t_\eta) \right] - (t_- p_+^\mu - t_+ p_-^\mu) \right\} \frac{\partial^2 A(x, y)}{\partial x^2} \\
&- \frac{3\sqrt{3}}{M_\eta^2 Q^2} (t_\eta p_0^\mu - t_0 p_\eta^\mu) \frac{\partial^2 A(x, y)}{\partial x \partial y} + \mathcal{O}(k).
\end{aligned} \tag{8}$$

If one uses the experimental amplitude as given by the Dalitz plot distribution (4) the last term in (8) involving $\frac{\partial^2 A(x, y)}{\partial x \partial y}$ will in fact not contribute. As already announced, we use for the slope parameters the experimental values [9,12] $a = -1.22 \pm 0.07$, $b = 0.22 \pm 0.11$ and the theoretical prediction [4] $c = 0.10$. The results for the rate normalized to $\Gamma(\eta \rightarrow \pi^+\pi^-\pi^0)$ are given in Table 2 for five bins in the photon energy E_γ (in the η rest frame).

| E_γ (MeV) | $\Gamma_{\text{GB}}(\eta \rightarrow \pi^+\pi^-\pi^0\gamma)/\Gamma(\eta \rightarrow \pi^+\pi^-\pi^0)$ |
|------------------|---|
| 10–30 | $(2.30 \pm 0.04) \times 10^{-3}$ |
| 30–50 | $(5.99 \pm 0.10) \times 10^{-4}$ |
| 50–70 | $(1.85 \pm 0.04) \times 10^{-4}$ |
| 70–90 | $(4.47 \pm 0.11) \times 10^{-5}$ |
| > 90 | $(5.00 \pm 0.14) \times 10^{-6}$ |

Table 2: Rates for $\Gamma(\eta \rightarrow \pi^+\pi^-\pi^0\gamma)$ with the GB amplitude (8) for different bins in the photon energy E_γ , normalized to $\Gamma(\eta \rightarrow \pi^+\pi^-\pi^0)$.

The relative branching ratios for $E_\gamma \geq 10$ and 50 MeV, respectively are

$$\begin{aligned}
B(\eta \rightarrow \pi^+\pi^-\pi^0\gamma; E_\gamma \geq 10 \text{ MeV})_{\text{GB}} &= (3.14 \pm 0.05) \times 10^{-3} B(\eta \rightarrow \pi^+\pi^-\pi^0) \\
B(\eta \rightarrow \pi^+\pi^-\pi^0\gamma; E_\gamma \geq 50 \text{ MeV})_{\text{GB}} &= (2.35 \pm 0.05) \times 10^{-4} B(\eta \rightarrow \pi^+\pi^-\pi^0).
\end{aligned}
\tag{9}$$

The errors given in both (9) and Table 2 are due to the experimental errors of the slope parameters a, b . These errors would of course be much larger if we would not normalize to $\Gamma(\eta \rightarrow \pi^+\pi^-\pi^0)$.

We can now make a first comparison with the work of Ref. [8]. Bramon et al. constructed a simple approximation to the Low amplitude (7). They dropped the derivative term in (7) and took instead the amplitude $A(x, y)$ of $\mathcal{O}(p^4)$ [3] at the center of the Dalitz plot. In fact, they did not exactly use the amplitude of Ref. [3] but increased the counterterm amplitude to account for the discrepancy between the experimental rate and the predicted rate of $\mathcal{O}(p^4)$. With these assumptions, they obtain [8]

$$\begin{aligned}
B(\eta \rightarrow \pi^+\pi^-\pi^0\gamma; E_\gamma \geq 10 \text{ MeV})_{\text{bremsstrahlung}} &= 2.81 \times 10^{-3} B(\eta \rightarrow \pi^+\pi^-\pi^0) \\
B(\eta \rightarrow \pi^+\pi^-\pi^0\gamma; E_\gamma \geq 50 \text{ MeV})_{\text{bremsstrahlung}} &= 1.85 \times 10^{-4} B(\eta \rightarrow \pi^+\pi^-\pi^0)
\end{aligned}
\tag{10}$$

In spite of the rather drastic approximations made, this prediction is quite close to our result (9) that is based on the GB amplitude (8) and on experimental input for the slope parameters. Of course, it is difficult to assign an error to the prediction of Bramon et al. With the errors given in (9) due to the experimental errors of the slope parameters, our prediction for $B(\eta \rightarrow \pi^+\pi^-\pi^0\gamma; E_\gamma \geq 10 \text{ MeV})$ is more than 6 standard deviations bigger than that of Ref. [8]. The discrepancy increases for larger values of the cut in the photon energy.

Before attributing any significance to the predictions (9), we will of course have to investigate the direct emission amplitude. Before doing so, we compare the rates for the GB amplitude (8) with the ones for the Low amplitude (7) in the same photon energy bins

| E_γ (MeV) | $(\Gamma_{\text{GB}} - \Gamma_{\text{Low}})/\Gamma_{\text{GB}}$ |
|------------------|---|
| 10–30 | 2.0×10^{-3} |
| 30–50 | 8.7×10^{-3} |
| 50–70 | 1.9×10^{-2} |
| 70–90 | 3.3×10^{-2} |
| > 90 | 4.9×10^{-2} |

Table 3: Relative differences in the rates between GB and Low. Listed are the quantities $\int_{E_\gamma^{(1)}}^{E_\gamma^{(2)}} \left(\frac{d\Gamma_{\text{GB}}}{dE_\gamma} - \frac{d\Gamma_{\text{Low}}}{dE_\gamma} \right) dE_\gamma \bigg/ \int_{E_\gamma^{(1)}}^{E_\gamma^{(2)}} \frac{d\Gamma_{\text{GB}}}{dE_\gamma} dE_\gamma$ for different bins in the photon energy.

as before. The results displayed in Table 3 show that the differences are rather small in all energy bins. This is due to the fact that $E_{\text{GB}}^\mu - E_{\text{Low}}^\mu$ is only sensitive to the quadratic slope parameter c in (4), numerically the smallest of the three parameters. Nevertheless, the difference between GB and Low is still bigger than the one-loop contribution to the direct emission amplitude to which we now turn.

3. The full radiative amplitude is the sum of the GB amplitude (8) and of a direct emission amplitude E_{DE}^μ :

$$E^\mu = E_{\text{GB}}^\mu + E_{\text{DE}}^\mu . \quad (11)$$

In this paragraph we calculate the direct emission amplitude of $\mathcal{O}(p^4)$. As shown in Ref. [6], E_{DE}^μ has the following general structure at this order:

$$E_{\text{DE}}^\mu = E_{\text{counterterm}}^\mu + \sum_{\text{loops}} (\Delta^\mu + H^\mu) . \quad (12)$$

As already mentioned, there is no counterterm contribution to direct emission for $\eta \rightarrow \pi^+ \pi^- \pi^0 \gamma$. The (finite) loop contribution is exclusively due to diagrams of the topology shown in Fig. 1 where a photon should be appended to all charged lines and all vertices with at least two charged fields.

The loop amplitude consists of a sum of two gauge invariant parts (for each loop diagram) Δ^μ and H^μ . Referring to Ref. [6] for details, we recall that both Δ^μ and H^μ depend only on the on-shell couplings of the vertices V_1, V_2 in Fig. 1. Those vertices have the general form in momentum space

$$\begin{aligned} V_1 &= a_0 + a_1 p_a \cdot p_b + a_2 p_a \cdot x \\ &\quad + a_3 (x^2 - M_x^2) + a_4 (y^2 - M_y^2) + a_5 (p_a^2 - M_a^2) + a_6 (p_b^2 - M_b^2) \\ V_2 &= b_0 + b_1 p_c \cdot p_d + b_2 p_c \cdot x \\ &\quad + b_3 (x^2 - M_x^2) + b_4 (y^2 - M_y^2) + b_5 (p_c^2 - M_c^2) + b_6 (p_d^2 - M_d^2) . \end{aligned} \quad (13)$$

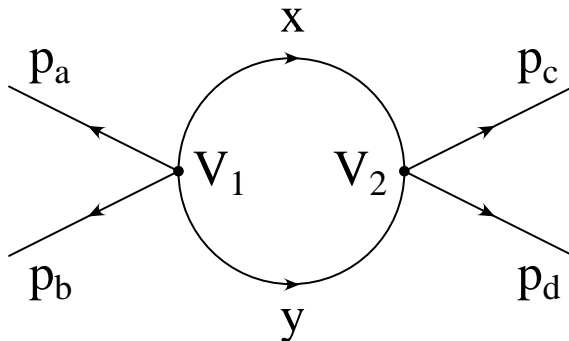


Figure 1: One-loop diagram for the general four-meson transition. For the radiative amplitude, the photon must be appended to every charged meson line and to every vertex with at least two charged fields. The vertices V_1, V_2 are defined in Eq. (13).

The relevant on-shell coefficients for the various diagrams are collected in Table 4. We have included the diagrams with two neutral intermediate particles for completeness although they do not contribute to either Δ^μ or H^μ here. In general, H^μ is always zero in this case but Δ^μ may be non-zero depending on the assignment of particle labels.¹

The $\eta \rightarrow 3\pi$ couplings vanish of course for $m_u = m_d$. In contrast to Ref. [8], we keep the pion loop contributions since they turn out to be comparable in magnitude to the kaon loops which we calculate in the isospin limit. The main contribution of direct emission arises in the interference with the GB amplitude (8). The corresponding contributions to the rate, separately for pions and kaons, are shown in Table 5.

Although pion and kaon loops make comparable contributions to the rate their impact is quite small for almost all photon energies. Integrating the differential rate over the photon energy for $E_\gamma \geq 10$ MeV produces a correction to the branching ratio that is smaller than the error given in (9) for the GB contribution only. It is even slightly below the difference between the rates for GB and Low amplitudes for most photon energies (cf. Table 3). The relative size of the loop amplitude increases with E_γ^{\min} at the expense of decreasing rates.

For the loop contributions to direct emission we only agree with Ref. [8] to the extent that they are small. Bramon et al. did not include the pion loops and they did not calculate the interference with the dominating bremsstrahlung amplitude. Taking the kaon loop amplitude by itself leads of course to a very small rate that is completely negligible [8] in comparison with the interference term.

¹In fact, the loop contribution to Δ^μ with two π^0 in the loop was missed in the calculation of $K_L \rightarrow \pi^+\pi^-\pi^0$ [7]. The change in the rate is numerically insignificant.

Table 4: On-shell coefficients of the vertices V_1, V_2 defined in (13) for the various loop diagrams in units of $1/F^2$ and with $\overline{M}_1^2 = (m_d - m_u)B_0/(\sqrt{3}(M_\eta^2 - M_\pi^2))$.

| $\eta(-p_b) \rightarrow \pi_a(p_a)$ + $M_x(x)M_y(y)$ $\rightarrow \pi_c(p_c)\pi_d(p_d)$ | a_0 | a_1 | a_2 | b_0 | b_1 | b_2 |
|---|--|----------------------|---------------------|---------------------|---------------|------------|
| $\eta \rightarrow \pi^0 +$ $\pi^+ \pi^- \rightarrow \pi^+ \pi^-$ | $-\overline{M}_1^2(3M_\eta^2 - M_\pi^2)/3$ | $-2\overline{M}_1^2$ | 0 | $2M_\pi^2$ | 2 | -2 |
| $\eta \rightarrow \pi^0 +$ $\pi^0 \pi^0 \rightarrow \pi^+ \pi^-$ | $-\overline{M}_1^2(M_\eta^2 - M_\pi^2)$ | 0 | 0 | M_π^2 | 2 | 0 |
| $\eta \rightarrow \pi^+ +$ $\pi^0 \pi^- \rightarrow \pi^0 \pi^-$ | $4\overline{M}_1^2 M_\pi^2/3$ | $2\overline{M}_1^2$ | $2\overline{M}_1^2$ | M_π^2 | 0 | -2 |
| $\eta \rightarrow \pi^- +$ $\pi^0 \pi^+ \rightarrow \pi^0 \pi^+$ | $4\overline{M}_1^2 M_\pi^2/3$ | $2\overline{M}_1^2$ | $2\overline{M}_1^2$ | M_π^2 | 0 | -2 |
| $\eta \rightarrow \pi^0 +$ $K^- K^+ \rightarrow \pi^+ \pi^-$ | $M_\pi^2/(2\sqrt{3})$ | $\sqrt{3}/2$ | 0 | 0 | 0 | 1 |
| $\eta \rightarrow \pi^0 +$ $K^0 \overline{K}^0 \rightarrow \pi^+ \pi^-$ | $-M_\pi^2/(2\sqrt{3})$ | $-\sqrt{3}/2$ | 0 | 0 | 0 | 1 |
| $\eta \rightarrow \pi^+ +$ $K^0 K^- \rightarrow \pi^0 \pi^-$ | $M_\pi^2/\sqrt{6}$ | $\sqrt{\frac{3}{2}}$ | 0 | $-M_\pi^2/\sqrt{2}$ | $-1/\sqrt{2}$ | $\sqrt{2}$ |
| $\eta \rightarrow \pi^- +$ $\overline{K}^0 K^+ \rightarrow \pi^0 \pi^+$ | $M_\pi^2/\sqrt{6}$ | $\sqrt{\frac{3}{2}}$ | 0 | $-M_\pi^2/\sqrt{2}$ | $-1/\sqrt{2}$ | $\sqrt{2}$ |

4. Since there is no counterterm contribution to direct emission at $\mathcal{O}(p^4)$ resonance exchange can only enter at $\mathcal{O}(p^6)$. Actually the $SU(2)$ -singlet nature of the η field implies that most of the resonance contributions vanish also at $\mathcal{O}(p^6)$. The only relevant direct emission amplitude surviving at this order is generated through the product of the following $\mathcal{O}(p^3)$ vector operators [14]:

$$\mathcal{L}_V = h_V \varepsilon_{\mu\nu\rho\sigma} \langle V^\mu \{ u^\nu, f_+^{\rho\sigma} \} \rangle + i\theta_V \varepsilon_{\mu\nu\rho\sigma} \langle V^\mu u^\nu u^\rho u^\sigma \rangle + \dots \quad (14)$$

The couplings in \mathcal{L}_V can in principle be determined from the phenomenology of vector meson decays. The decay rate for $\omega \rightarrow \pi^0 \gamma$ [9] fixes $|h_V| = 0.037$. For the second coupling θ_V , one has to rely on models for the time being. Hidden symmetry predicts $\theta_V = 2h_V$ [15], while the ENJL model [16] has $\theta_V = 0.050$. These values are compatible with each other and we will choose $\theta_V = 0.050 \div 0.075$ for the numerical estimate. We will also assume that the field V^μ in (14) describes a nonet of vector mesons with ideal mixing.

| E_γ (MeV) | $(\Gamma_{\text{GB+DE}} - \Gamma_{\text{GB}})/\Gamma_{\text{GB}}$ (pions) | $(\Gamma_{\text{GB+DE}} - \Gamma_{\text{GB}})/\Gamma_{\text{GB}}$ (kaons) |
|------------------|---|---|
| 10–30 | 4.5×10^{-4} | 6.4×10^{-4} |
| 30–50 | 2.7×10^{-3} | 2.7×10^{-3} |
| 50–70 | 8.4×10^{-3} | 5.9×10^{-3} |
| 70–90 | 2.1×10^{-2} | 9.9×10^{-3} |
| > 90 | 6.0×10^{-2} | 1.4×10^{-2} |

Table 5: Relative rate differences for the interference between GB and the one-loop contributions to direct emission. The notation is analogous to Table 3.

Integrating out the vector mesons in the Lagrangian (14), one obtains the following effective Lagrangian of $\mathcal{O}(p^6)$ for the direct emission in $\eta \rightarrow \pi^+ \pi^- \pi^0 \gamma$:

$$\mathcal{L}_{VMD}^6 = -\frac{64i h_V \theta_V F^{\mu\nu} \partial_\rho \eta}{3\sqrt{3} M_V^2 F_\pi^4} \left[\partial_\rho \pi^0 (\partial_\nu \pi^+ \partial_\mu \pi^-) + \partial_\mu \pi^0 (\partial_\rho \pi^+ \partial_\nu \pi^- - \partial_\rho \pi^- \partial_\nu \pi^+) \right]. \quad (15)$$

This Lagrangian gives rise to the decay amplitude

$$E_{\text{DE,VMD}}^\mu = -\frac{64 h_V \theta_V}{3\sqrt{3} M_V^2 F_\pi^4} [p_\eta \cdot p_0 g_{+-}^\mu + p_\eta \cdot p_- g_{0+}^\mu + p_\eta \cdot p_+ g_{-0}^\mu] \quad (16)$$

$$g_{ij}^\mu = t_i p_j^\mu - t_j p_i^\mu$$

which differs from formula (19) in [8].

For the values of h_V and θ_V in the range mentioned before, we find that this amplitude provides a contribution to the direct emission comparable or slightly larger in size than the one from the loops. In Table 6, we display the interference terms in the rate due to vector exchange alone (for $h_V \theta_V = 2.8 \times 10^{-3}$) and due to the total direct emission.

Due to the comparable size but opposite sign of loop and VMD contributions, the total direct emission in $\eta \rightarrow \pi^+ \pi^- \pi^0 \gamma$ turns out to be very small. If $h_V \theta_V$ is positive (as theoretically predicted) and in the expected range, it will be very difficult to observe any deviation from the GB prediction.

5. Our main results can be summarized as follows:

- i. The concept of generalized bremsstrahlung is very efficient in avoiding the propagation of uncertainties in the non-radiative decays to the direct emission amplitudes. In the case at hand, we have shown that the numerically important final state interactions in $\eta \rightarrow \pi^+ \pi^- \pi^0$ [4,5] are easily incorporated in the GB amplitude. This

| E_γ (MeV) | $(\Gamma_{\text{GB+DE}} - \Gamma_{\text{GB}})/\Gamma_{\text{GB}}$ (VMD) | $(\Gamma_{\text{GB+DE}} - \Gamma_{\text{GB}})/\Gamma_{\text{GB}}$ (total) |
|------------------|---|---|
| 10–30 | -1.3×10^{-3} | -0.1×10^{-3} |
| 30–50 | -1.0×10^{-2} | -4.9×10^{-3} |
| 50–70 | -3.4×10^{-2} | -2.0×10^{-2} |
| 70–90 | -7.6×10^{-2} | -4.5×10^{-2} |
| > 90 | -1.4×10^{-1} | -6.2×10^{-2} |

Table 6: Relative rate differences for the interference between GB and direct emission: VMD (for $h_V\theta_V = 2.8 \times 10^{-3}$) and total direct emission. The notation is analogous to Table 3.

allows for a very precise prediction of the radiative decay rate normalized to the non-radiative transition:

$$B(\eta \rightarrow \pi^+\pi^-\pi^0\gamma; E_\gamma \geq 10 \text{ MeV}) = (3.14 \pm 0.05) \times 10^{-3} B(\eta \rightarrow \pi^+\pi^-\pi^0). \quad (17)$$

- ii. The $\pi\pi$ loops in the direct emission amplitude, though isospin suppressed, are competitive with the $K\bar{K}$ loops. However, even the combined one-loop amplitude is negligible compared to GB for most of the photon energy range.
- iii. We find that vector meson exchange (in the expected range for the vector couplings) has comparable size but opposite sign of the loop contributions. If this model-dependent prediction is correct, we do not expect to observe any direct emission effect in $\eta \rightarrow \pi^+\pi^-\pi^0\gamma$, even with the anticipated yield of 10^8 η per year [10].

Acknowledgments

G.D. and G.I. wish to thank the Institute of Nuclear Theory (INT) of the Univ. of Washington for hospitality where part of this work has been done.

References

- [1] D.G. Sutherland, Phys. Lett. 23 (1966) 384;
J.S. Bell and D.G. Sutherland, Nucl. Phys. B 4 (1968) 315;
R. Baur, J. Kambor and D. Wyler, Nucl. Phys. B 460 (1996) 127.
- [2] H. Osborne and D.J. Wallace, Nucl. Phys. B 20 (1970) 23;
J.A. Cronin, Phys. Rev. 161 (1967) 1483.
- [3] J. Gasser and H. Leutwyler, Nucl. Phys. B 250 (1985) 539.
- [4] J. Kambor, C. Wiesendanger and D. Wyler, Nucl. Phys. B 465 (1996) 215.
- [5] A.V. Anisovich and H. Leutwyler, Phys. Lett. B 375 (1996) 335.
- [6] G. D'Ambrosio, G. Ecker, G. Isidori and H. Neufeld, Phys. Lett. B 380 (1996) 165.
- [7] G. D'Ambrosio, G. Ecker, G. Isidori and H. Neufeld, Z. Phys. C 76 (1997) 301.
- [8] A. Bramon, P. Gosdzinsky and S. Tortosa, Phys. Lett. B 377 (1996) 140.
- [9] Review of Particle Physics, C. Caso et al. (Particle Data Group), Eur. Phys. J. C 3 (1998) 1.
- [10] The Second DAΦNE Physics Handbook, Eds. L. Maiani, G. Pancheri and N. Paver (Servizio Documentazione INFN, Frascati, 1995).
- [11] J. Gasser and H. Leutwyler, Nucl. Phys. B 250 (1985) 465.
- [12] A. Abele et al., Phys. Lett. B 417 (1998) 197.
- [13] F.E. Low, Phys. Rev. 110 (1958) 974.
- [14] G. Ecker, J. Gasser, H. Leutwyler, A. Pich and E. de Rafael, Phys. Lett. B 223 (1989) 425.
- [15] M. Bando, T. Kugo, K. Yamawaki, Phys. Rep. 164 (1988) 217.
- [16] J. Prades, Z. Phys. C 63 (1994) 491.